ACS APPLIED MATERIALS & INTERFACES

Research Article

www.acsami.org

Highly Durable and Efficient Quantum Dot-Sensitized Solar Cells Based on Oligomer Gel Electrolytes

Heejin Kim, Insung Hwang, and Kijung Yong*

Surface Chemistry Laboratory of Electronic Materials (SCHEMA), Department of Chemical Engineering, Pohang University of Science and Technology (POSTECH), Pohang 790-784, Korea

ABSTRACT: For stable quantum dot-sensitized solar cells, an oligomer-contained gel electrolyte was employed with a carbon-based counter electrode and a hierarchically shelled ZnO photoelectrode. Poly(ethylene glycol) dimethyl-ether (PEGDME) was added to the polysulfide electrolyte to enhance the stability of the methanol-based electrolyte. In addition, the nanocomposite gel electrolyte with fumed silica was used, which provided a solid three-dimensional network. A quantum-dot-modified ZnO nanowire photoanode enhanced the visible light harvesting, and a Pt/CNT-RGO counter electrode increased the catalytic activity. The oligomer gel electrolyte prevented the liquid electrolyte from leaking, and the carbon-based counter electrode retarded chemical poisoning at the counter electrode. The optimized cell exhibited 5.45% photoelectric conversion efficiency with long-term stability demonstrated over 5000 s operation time.

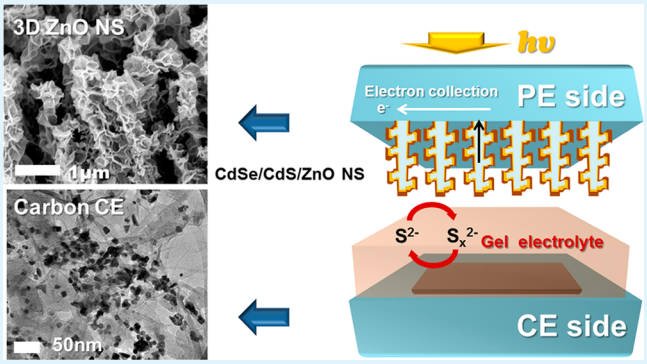

KEYWORDS: *quantum dot-sensitized solar cell, ZnO, gel electrolyte, CdS, CdSe, oligomer*

INTRODUCTION

Quantum dot-sensitized solar cells (QDSSCs) have attracted much attention as alternative photovoltaic devices that have a photon-to-electric conversion mechanism similar to that of dye-sensitized solar cells (DSSCs).[1−5] The main advantages of QDSSCs are photoelectric conversion in the full visible light range, higher electron collection efficiency, and low cost of fabrication.[6,7] Many attempts have been made to increase the light harvesting efficiency of QDSSCs through the deposition of various quantum dot semiconductor nanocrystals such as CdS,[8,9] CdSe,[5,10] and PbS.[11−13] The semiconductor quantum dots, which act as visible light harvesting materials, have the potential to demonstrate several especially advantageous properties, including the quantum confinement effect, high absorption, and the generation of multiple electron carriers.[3] Co-sensitizing devices using CdS and CdSe have been the special interest of many researchers because these devices can absorb the entire visible light spectrum and separate the photoexcited electron−hole pairs through their type II cascade band structure.[10,14] Furthermore, the nanostructured photoelectrode used for quantum dot deposition plays an important role in electron transport and collection. Although mesoporous TiO_2 nanostructures have been widely used as photoelectrodes due to their high surface area for sensitizer deposition,[15,16] one-dimensional ZnO can also be a potential candidate because its structure can provide a direct electron pathway for more efficient electron transport.[11,17,18] In addition, ZnO has a potential application as a photoelectrode due to its higher electron mobility value as compared to that of TiO_2 (205−1000 $cm^2\ V^{-1}\ s^{-1}$ for ZnO and 0.1−4 $cm^2\ V^{-1}\ s^{-1}$ for TiO_2).[18,19] Furthermore, the lower surface area of the one-dimensional ZnO nanowire arrays can be overcome through secondary lateral growth on the on-dimensional nanostructure surface.[20] In particular, the three-dimensional ZnO nanostructures in this study enable efficient charge collection because they consist of a one-dimensional ZnO nanowire at the core and a two-dimensional ZnO nanosheet on the core surface.[21] This composition can provide higher quantum dot loading and higher electron transport, thereby leading to higher charge collection efficiency. On the basis of these materials, we examined the highly efficient QDSSCs that had a photoelectric conversion efficiency of approximately ∼5% under 1 sun irradiation, as described in previous research.[21]

However, another important property of QDSSCs that requires further research for practical application is their durability. In general, QDSSCs use a polysulfide redox relay-based electrolyte and gold-deposited counter electrode assemblies.[22,23] Despite the high conversion efficiency of QDSSCs, photovoltaic devices that employ a liquid electrolyte have the potential for other problems, including leakage, volatility, flammability, and quantum dot corrosion.[24−26] Thus, the presence of liquid electrolyte in conventional devices may also result in some practical limitations for sealing and long-term stability. A nonliquid electrolyte is necessary for ideally

Received: March 11, 2014
Accepted: July 2, 2014
Published: July 2, 2014

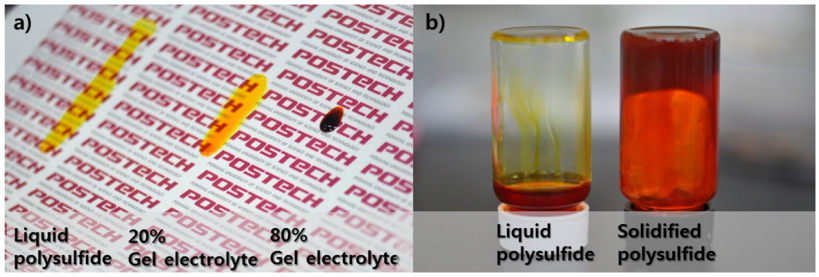

Figure 1. Digital images of the gel electrolytes with various compositions. (a) The comparison of the viscosity and volatility of PEO-based oligomer at varying concentration (liquid electrolyte and 20 vol %, 80 vol % of the PEO-based oligomer concentrations). (b) The comparison of the liquid and solidified electrolyte with silica nanofiller additives.

durable sensitized solar cells. There have been many attempts to replace the electrolyte in solid-state sensitized solar cells with alternatives such as inorganic hole transport materials,[27,28] organic p-type polymer hole transporting materials,[29−31] polymer included redox coupled electrolyte,[32−35] and nanocomposite gel electrolytes.[34,36−38] In previous research, we proposed p-type conjugated polymer (P3HT) imbedded QDSSCs for a solid-state solar cell device with a 1.5% photoelectric conversion efficiency.[30] However, the device has a limited photovoltaic performance due to the pore filling of the photoelectrode interspacing. To improve this limitation, we have adopted the modified electrolyte containing oligomer solvent and fumed silica nanocomposite in the polysulfide electrolyte.[39−41] The oligomer polymer solvent is poly(ethylene glycol)dimethyl-ether (PEGDME) (M_w = 500 g mol^{-1}), which contains oxygen atom polar ligands for dissolving the redox couple. By substituting some of the solvent with oligomer, the volatility and flammability caused by methanol-based electrolyte can be improved. Moreover, fumed silica was used as the nanofiller for solidification, thus providing physical strength and light scattering properties. In addition, the standard gold deposited counter electrode was replaced with a carbon-based counter electrode consisting of a carbon nanotube (CNT), reduced graphene, and Pt nanoparticles. Using this material, the typical interfacial chemical reaction on the gold surface can be efficiently retarded, resulting in higher endurance.[42] Thus, the durable and high photon-to-electric conversion efficiency was obtained in this study, and the resultant photoelectric efficiency was 5.45% at 1 sun irradiation. The cell also exhibited enhanced durability over 5000 s operation at 1 sun irradiation.

EXPERIMENTAL SECTION

Fabrication of Photoelectrodes. CdSe-/CdS-deposited three-dimensional ZnO nanostructures were fabricated for the photoelectrodes using the hydrothermal method. At first, the ZnO nanowire arrays were grown on F-doped tin oxide (FTO) glass (TEC, 8 Ω/□) by an ammonia solution method.[43] Using the ZnO target, the patterned 50 nm ZnO film was deposited on FTO glass, and the substrate was immersed in an aqueous solution containing 10 mM $Zn(NO_3)_2{\cdot}6H_2O$ with pH 11 conditions, which was adjusted in ammonia solution (28 wt % in water). The solution was heated at 95 °C for 12 h until the ZnO nanowire arrays grew to approximately 10 μm. Subsequently, the ZnO nanowire grown FTO glass was transferred to an aqueous solution of 10 mM $Zn(NO_3)_2{\cdot}6H_2O$, 10 mM hexamethyltetramine, and 1 mM trisodium citrate at 70 °C for 9 h.[21] After the ZnO nanostructure growth, the CdS and CdSe were deposited using solution reactions.[8,44] The successive ionic layer absorption and reaction (SILAR) process for the CdS deposition was conducted using 20 cycles. The electrode was first briefly dipped in a 200 mM $CdSO_4$ aqueous solution for 30 s, rinsed with deionized water for 30 s, dipped in aqueous 200 mM Na_2S solution for 30 s, and finally rinsed with water for 30 s. This in situ deposition process was repeated for 20 cycles with the desirable 10 nm CdS shell size on the ZnO surface. After that, the CdSe was deposited using a chemical bath deposition (CBD) process. The electrode was immersed in 2.5 mM $Cd(CH_3COO)_2$, 0.25 M Na_2SeSO_3, and 45 mM NH_4OH at 95 °C for 3 h. The process was repeated three times until the desirable CdSe nanocrystal growth was achieved.[45]

Using the prepared photoelectrode, the sandwich QDSSC was assembled with a 0.25 mm^2 cell dimension. The carbon-based counter electrode was prepared using the previous recipe.[42] Briefly, the graphene oxide made using Hammer's methods and the CNT purchased from Hanwha nanotech (CM-95) were mixed in a 1:1 weight ratio and dispersed ultrasonically in ethanol (3 g/L). Subsequently, the $H_2PtCl{\cdot}6H_2O$ was added in solution with a 1:1 weight ratio, and 2 mL of HCl was added to the 10 mL solution. After stirring, the solution was centrifuged and washed twice with ethanol. The prepared mixture was then spray coated on FTO glass in isopropyl alcohol dispersed solution (1 g/L) at 120 °C.

Fabrication of Gel Electrolyte. To prepare the gel electrolyte, the poly(ethylene glycol)dimethyl-ether (PEGDME) (M_w = 500 g mol^{-1}) (Aldrich) was dissolved in a 7:3 (v/v) mixture of methanol and distilled water at various volume ratios until a uniform solution was formed. Next, 0.5 M Na_2S, 2 M S, and 0.2 M KCl were added into the solution. After the mixture was stirred at 60 °C, the fumed silica nanoparticles (15 nm, Aldrich) were added into polymer blend solution. The prepared gel electrolyte was stirred for 6 h at 60 °C.

Characterization. Scanning electron microscopy (SEM) images were recorded using a Phillips XL30S field emission SEM. An atomic scale analysis of the crystal structure was performed on a transmission electron microscope (JEM-2200FS, JEOL at NCNT, POSTECH). The optical absorbance of the samples was analyzed using a UV2501PC (SHIMADZU) spectrometer with an ISR-2200 integrating sphere attachment for diffuse reflection measurements. Photocurrent density−voltage characteristics of the cells were measured using a solar simulator (ABET, SUN3000). The power of the simulated light was calibrated to AM 1.5 (100 mW cm^{-2}) using a standard silicon solar cell (PV Measurement Inc.). Electrochemical impedance spectroscopy (EIS) experiments were characterized with symmetrical cells in the dark using a potentiostat (Ivium Technologies). A thin layer symmetric cell was fabricated by stacking two similar electrodes with Sulyn spacer and sealed by heating on a hot plate. The frequency range was used from 100 kHz to 100 mHz, with a modulation amplitude of 10 mV at 0 V bias voltage.

RESULTS AND DISCUSSION

To realize stable quantum dot-sensitized solar cells, a nonvolatile, inflammable electrolyte is necessary. For this reason, we substituted poly(ethylene oxide) (PEO) for the liquid electrolyte, which consists of methanol and water. PEO is a well-known conducting polymer that can be used as an electrolyte in dye-sensitized solar cells (DSSCs).[32,33,46,47] As the polymer solvent, PEO has electric conductivity as a result of excellent complexation with ionic salts due to the unpaired

electrons on the ether oxygen atoms functioning as donors for the alkali cations in salts. Although the PEO, which generally has a molecular weight of a few thousand, is widely used as a polymer solvent, solid-state PEO-based polymers can suffer from poor electrode−electrolyte contact, and the overall photon-to-power conversion performance can thus be reduced. For this reason, we employed the low molecular weight PEO for more efficient interfacial penetration in the nanostructured photoelectrode. For a better comparison, the digital images of the each electrolyte condition are shown in Figure 1a and b. Figure 1a shows the changes of the electrolyte properties including viscosity and volatility as a function of PEO oligomer concentration. Figure 1b exhibits a solidified polysulfide electrolyte with only silica nanocomposite additives to the liquid electrolyte. When the electrolyte consisted of methanol and water, the liquid electrolyte exhibited high volatility and fluidity. As PEO oligomer (PEGDME) concentration increased to 80 vol %, the electrolyte showed lower volatility and enhanced viscosity at room temperature. For the accurate comparison of the viscosity, we conducted the viscosity measurement under 297 K condition depending on the PEGDME vol % concentration. In Table 1, the viscosity

Table 1. Measured Viscosity Values of the PEGDME 500 Mixed Electrolyte at 297 K

PEGDME (vol %)	0	20	50	80
viscosity (mPa s)	3.44	9.13	15.6	28.1

increased gradually with PEGDME concentration. However, the solidified gel electrolyte could not be obtained with the application of PEGDME as only an additive because the oligomer PEGDME has liquidity coming from the low molecular weight as compared to that of high molecular weight polymer.[48] In the current study, a solidified gel electrolyte was prepared by employing fumed silica nanocomposite as a nanoparticle filler.[39,40] Silica nanoparticles are a widely used material because a nanoparticle filler in an electrolyte enables the electrolyte to form a network that increases gelation and solidification, as observed in Figure 1b.

For the optimized preparation of the gel electrolyte, we examined the changes of the electrolyte properties. First, we compared the electrical properties of the electrolyte with the concentration of PEGDME. In this measurement, the PEGDME with 500 g mol^{-1} was substituted with a mixture of methanol and water solvent with various volume concentrations. When it is compared in Figure 2a, the ionic conductivity of gel electrolyte was relatively lower than liquid electrolyte (0%) due to the lower ionic conductivity of the oligomer PEO ($\sim 10^{-3}$ S cm^{-1}) as compared to that of the methanol, water mixture ($\sim 10^{-2}$ S cm^{-1}).[33] The characteristics of electrolytes were also examined in EIS analysis using the symmetric cell consisting of Au CE/electrolyte/Au CE. With the EIS spectra of symmetric cells, we could analyze the two semicircles attributed to the charge transfer at the counter/electrolyte interface and diffusion of ions in the electrolyte. The semicircle that indicates the charge transfer at the counter electrode (in the kHz range) was not observed due to the high radius semicircle at the low frequency region related to the diffusivity of the electrolytes. For this reason, we simply compared the radius of the semicircle with the assumption that the charge transport resistance is equal because the counter electrode was fixed in this experiment.[49,50] In Figure 2b, from the semicircle radius, we could compare the conductivity of the electrolyte consisting of various concentrations of PEO oligomer (PEDGME) and methanol/water mixture. As shown in Figure 2b, the internal resistance showed a larger radius for the semicircle, and indicates that the gel electrolyte has the lower ionic conductivity. The results exhibited the same trend as Figure 2a in that ionic conductivity was lowered as the concentration of PEO oligomer increased.

Using the same electrolytes as Figure 2, we fabricated the QDSSC cells. Figure 3 shows time-dependent photoresponse parameters of the PEGDME-contained electrolyte-based quantum dot coupled ZnO nanostructures for the various concentrations of PEGDME. In the QDSSC system, we used the three-dimensional ZnO nanostructured photoelectrode modified by the CdS and CdSe quantum dots. Using the Au deposited counter electrode, the cell exhibited ~4.68% photon-to-current conversion efficiency with the methanol/water mixed polysulfide electrolyte under 1 sun irradiation at the 5 mm × 5 mm cell size. When the PEO oligomer (PEDGME)-based gel electrolyte was adapted to the QDSSCs, there was not a remarkable change under a 20 vol % PEO oligomer ratio electrolyte. Basically, the current density is dependent on the ionic conductivity. However, 20 vol % PEO oligomer-based gel electrolyte showed an unusual current value measured as compared to that of liquid electrolyte. In Figure 2, 20% PEGDME electrolyte showed slightly lower conductivity than did the liquid electrolyte, which can result in lower redox couples and the associated reactions at the electrolyte/photoelectrode interface. In detail, a higher concentration of the redox couples might increase the side effect of the recombination of the electrons injected in the photoelectrode, thereby reducing the open circuit values.[47,51] When comparing

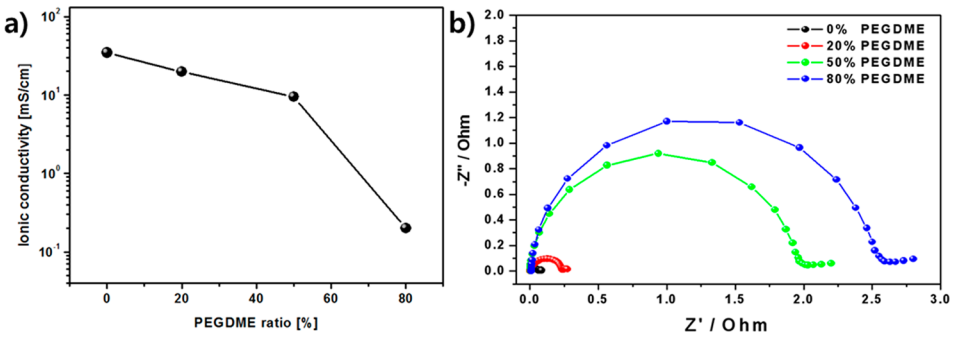

Figure 2. Comparison of the (a) ionic conductivity and (b) electrochemical impedance spectroscopy (EIS) analysis data of the symmetric cell (Au/electrolyte/Au) with various PEGDME concentrations.

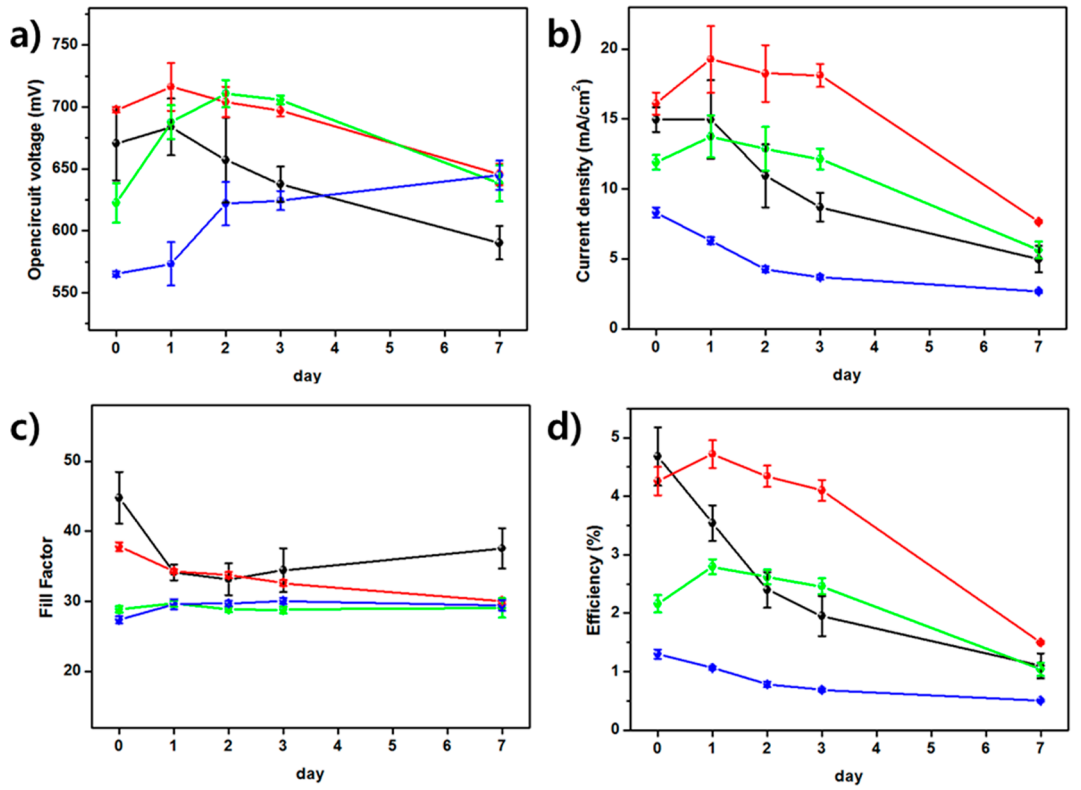

Figure 3. Time-dependent photoresponse parameters ((a) open circuit voltage, (b) current density, (c) fill factor, (d) efficiency) of the PEGDME-containing electrolyte-based quantum dot coupled 3D ZnO nanostructures for various concentrations of PEGDME (black: liquid electrolyte; 20, 50, and 80 vol % are red, green, and blue, respectively).

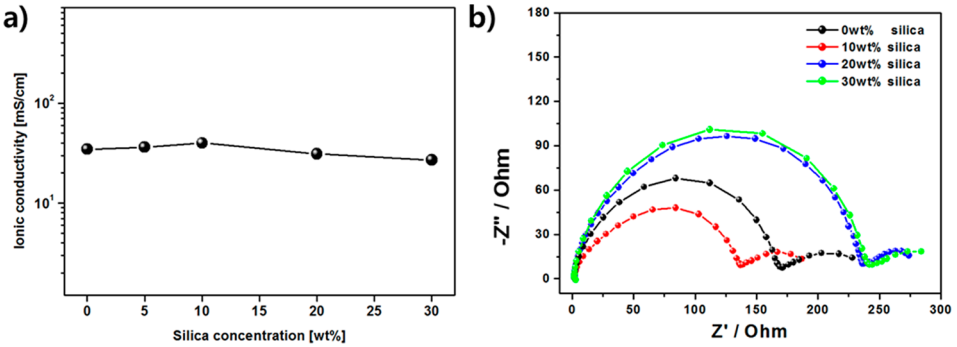

Figure 4. Comparison of the (a) ionic conductivity and (b) electrochemical impedance spectroscopy (EIS) analysis data of the symmetric cell (Au/electrolyte/Au) with various silica concentrations.

the 20% electrolyte with that of liquid electrolyte, the current density exhibited enhancement, although the modified electrolyte showed lower ionic conductivity and diffusivity. Thus, we assume that the lower ionic conductivity with comparable values ($\sim 10^{-2}$ S cm^{-1}) results in the lowering of the interfacial recombination ratio in the charge generation process. However, over the 20 vol % concentration of PEO oligomer (PEDGME) electrolyte, the low ionic conductivity influences the cell performance primarily through changes in the current density. In addition, the effect of the gel electrolyte can be distinguished in time-dependent cell performances. This is mainly due to the change in the electrolyte properties such as volatility and flammability. Although the fabricated cell was sealed with the cover glass and Surlyn, the cells may suffer from the electrolyte leakage and corrosiveness in the fabrication process. As time goes by, the fabricated cell degraded rapidly in liquid electrolyte. Although the cells employing a high PEO gel electrolyte ratios enhanced durability, the lower overall cell performance was not adequate for practical utilization. Thus, we have optimized the PEO composition of the gel electrolyte to the 20 vol % in the QDSSC system. However, the desired gel electrolyte was not suitable for solidified QDSSC because they still have lower viscosity and flammability due to the lower molecular weight oligomer PEO.

For this reason, we used the silica nanocomposite additives to the 20 vol % PEO electrolyte solution. There are many nanomaterials used for the nanofiller such as silica nanoparticles and TiO_2,[51,52] but silica is commonly used as a nanocomposite to solidify the electrolyte.[38,49] Silica nanoparticles efficiently decrease the crystallinity of the polymer and provide free volume in the electrolyte, resulting in enhanced ionic diffusivity. Specifically, the silica nanoparticles facilitate solidifying the

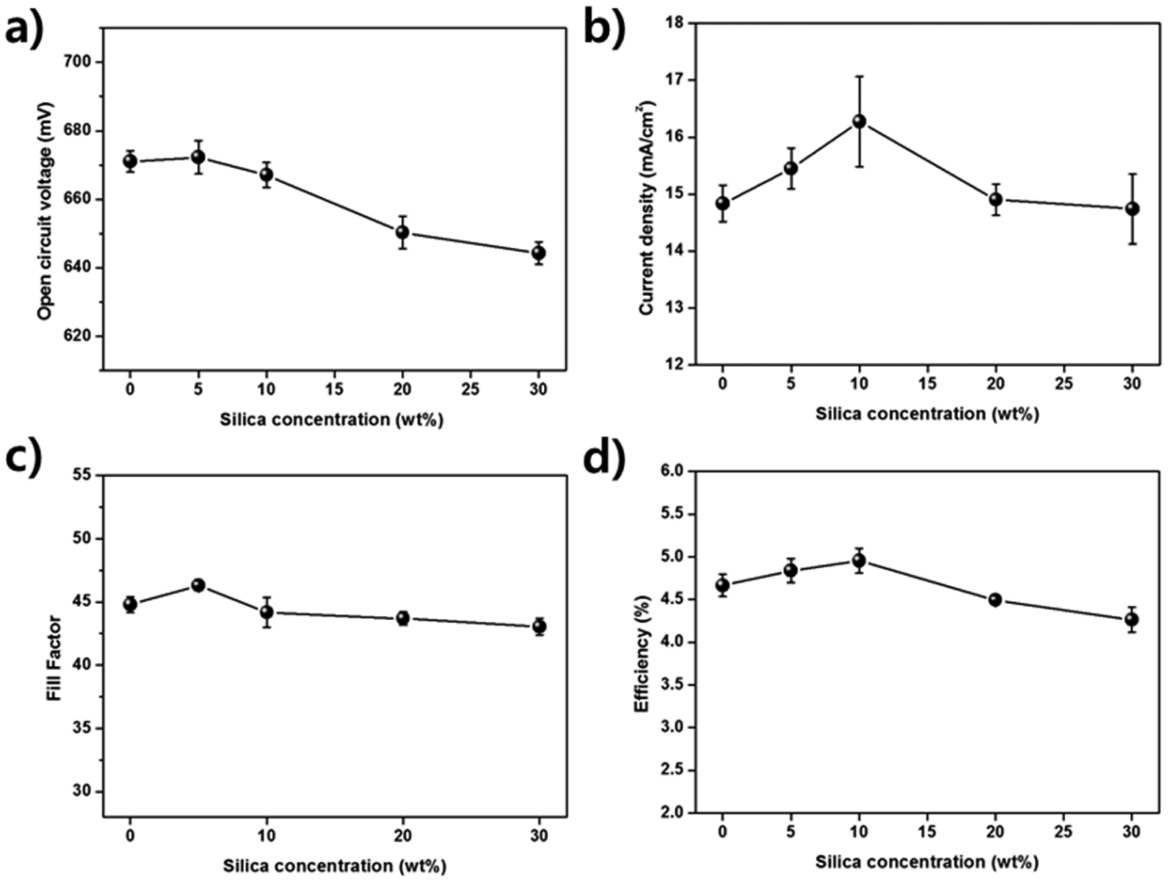

Figure 5. Silica concentration versus photoresponse parameters ((a) open circuit voltage, (b) current density, (c) fill factor, (d) efficiency) of QDSSCs based on quantum-dot-coupled 1D ZnO nanostructures.

electrolyte by attractive forces between the silica particles. It has been reported that silica nanoparticles can scatter incident light within the embedded electrolyte, which also affects the current density. In the current study, we employed the silica for solidifying the electrolyte in various concentrations. As shown in Figure 4, apparently ionic conductivity is not dependent on silica concentration, but the ionic conductivity was slightly enhanced at 10 wt % silica concentration. The ionic conductivity increased with the silica concentration until 10 wt %, followed by a decrease. This result can be explained by the conjecture that the optimum concentration of the silica provides the channel for the charge freely with the gel network and efficient transport of the redox couple. That is, the cations of the electrolyte can adsorb on the silica surface (Si−OH) and consequently enhance the anion redox couple mobility in the gel electrolyte.[40,49] However, they can hinder the transport of the redox couples in the electrolyte or interfacial reaction at the photoelectrode surface at concentrations above the optimum. This charge diffusivity also can be observed in an EIS analysis of the Au CE/electrolyte/Au CE symmetric cells. Except the 10 wt % silica concentration, the other higher concentrations showed increased internal resistance, as shown in Figure 4b.

This trend can also be observed in photo response parameters in the QDSSC system. In this measurement, all cells were fabricated with CdSe/CdS-deposited 1D ZnO nanostructured photoelectrode and Au-deposited counter electrode. The electrolyte was the 20 vol % PEO-based gel electrolyte as optimized in previous experiment. As expected, the cell showed maximum values in photocurrent density as depicted in Figure 5b. This result is mainly due to the enhanced ionic conductivity and diffusivity of the electrolyte, and it is assumed that the gel electrolyte with added nanocomposite also efficiently scatters the incident light. Although there are many assumptions that the nanocomposites can retard the interfacial recombination ratio because the nanoparticle lowers the redox couple contact area, the enhancement of the open circuit voltage that relates to the recombination ratio is not remarkable (Figure 5a). As compared to the fill factor, which is related to the electron transport resistance and shunt resistance (Figure 5c), there was no trend in the function with silica concentration. Although there was an enhancement at the point of 5 wt %, it may be related to the reduced interfacial contact area at the electrolyte and photoelectrode due to the adsorption of the silica nanoparticles. This result can be explained by the slight increase of the open circuit values in Figure 5a. From these results, we concluded that the 10 wt % silica nanocomposite is the optimum concentration in photo response performance as well as giving solidification.

The other important element in providing stability is the counter electrode as well as the electrolyte. Generally, the QDSSC applies the Au-deposited counter electrode for the electron injection to the redox couples, but the poisoning of the Au electrode can degrade the stability of the cell, as shown in the above results.[42] In this study, we employed the carbon-based counter electrode instead of the Au-deposited electrode. As observed in Scheme 1, the sandwich assembled QDSSC system consists of the three main components. The three-dimensional ZnO nanostructured photoelectrode was used for

Scheme 1. Schematic Image of the CdSe/CdS/ZnO Nanostructure-Based QDSSC Sandwich Cell Using the Carbon-Based Counter Electrode with the Polysulfide Gel Electrolyte and the Corresponding Electrode Images

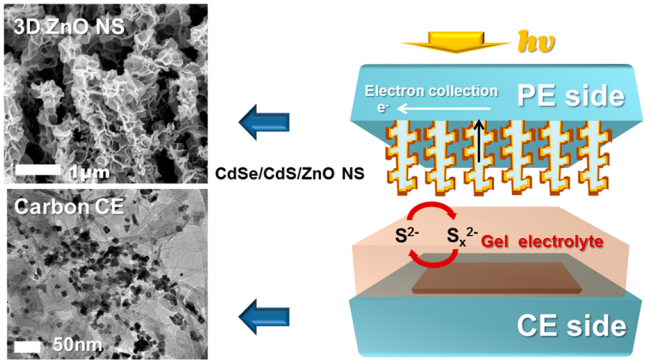

efficient light harvesting and charge generation. With the CdS and CdSe cosensitization, which can absorb the visible light over 750 nm, they can generate a high current density over 15 mA cm^{-2} under 1 sun irradiation. The Pt/CNT-RGO sprayed counter electrode was employed for the counter electrode, which mainly plays a role in electron injection to the electrolyte. With the 1D CNT and 2D RGO, the 3D components facilitate the efficient fast charge transport and the large surface as well as high electrical conductivity. In addition, the nanosized Pt noble metal was anchored on the 3D carbon support, giving enhanced electrocatalytic activity. This carbon-based counter electrode (CE) was fabricated according to our previous research, and it exhibited enhanced performance over the Au-deposited counter electrode. Specifically, the carbon-based CEs exhibited the enhanced stability because they efficiently retard the chemical reaction mainly occurring at the noble metal surface. Although the carbon-based CEs use the nanosized Pt noble metal, the chemical reaction with the redox couple is insignificant due to the lower amount of the noble metal as compared to the Au counter electrode. The comparison of cell performances for variant component-based cells was performed, and the results are shown in Figure 6. Using the carbon-based counter electrode, the cell showed the enhanced photo response performance with 5.69% photon-to-current conversion efficiency, which is enhanced as compared to an Au CE cell (5.09%). This value represents the enhanced electrocatalytic activity of the carbon-based counter electrode over the Au-deposited reference electrode. Subsequently, we employed the gel electrolyte to the 3D ZnO nanostructured photoelectrode and the carbon-based counter electrode (Figure 6b). The cell exhibited comparable photo response parameters, with 5.45% photon-to-electric conversion efficiency with a liquid electrolyte cell (Table 2). As mentioned above, we have considered two factors in stable QDSSC system. The first factor

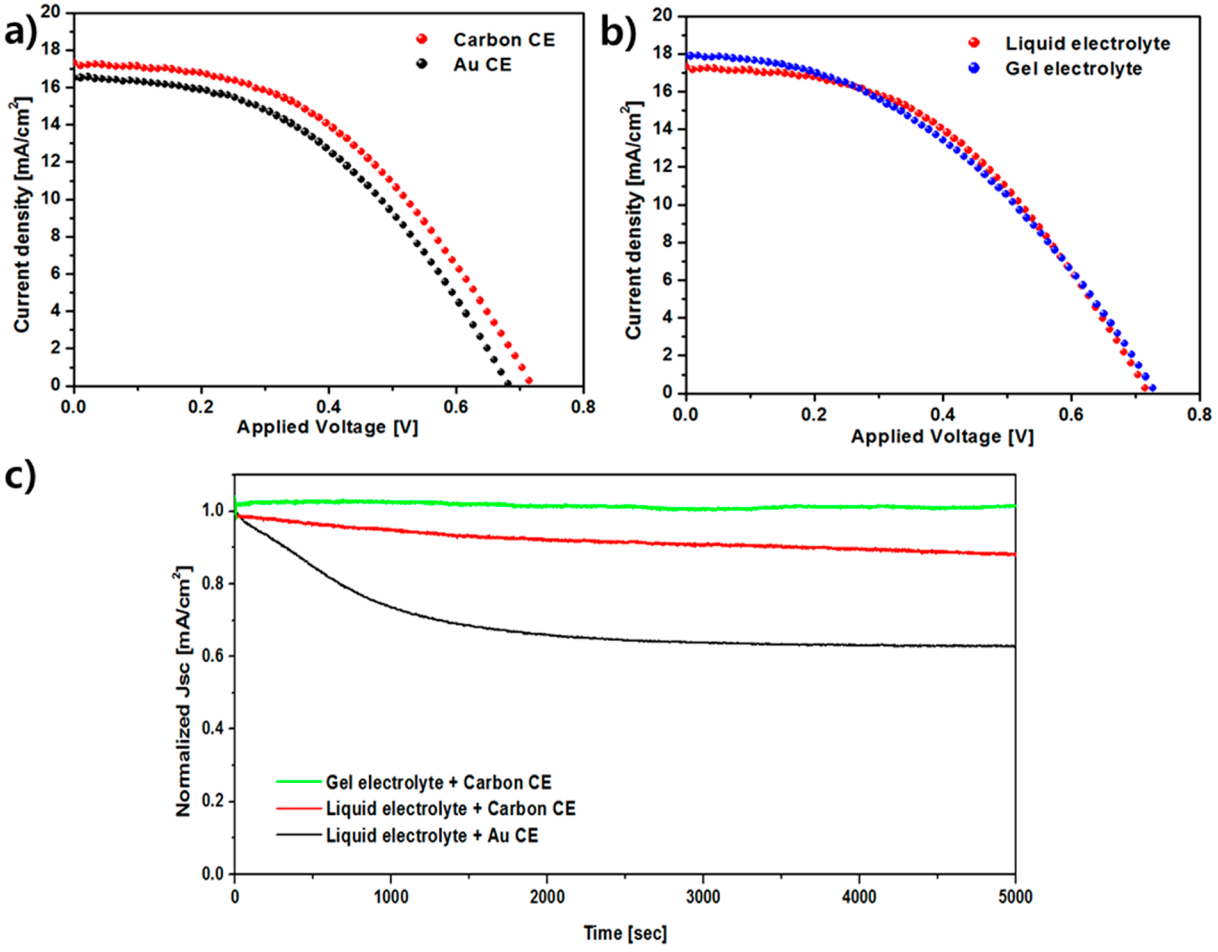

Figure 6. (a,b) *J*–*V* curves of the 3D ZnO-based QDSSCs with (a) carbon-based counter electrode versus Au counter electrode (liquid electrolyte) and (b) gel and liquid electrolyte using carbon-based counter electrode. (c) Normalized time-to-current analysis with different conditions.

Table 2. $J-V$ Curve Parameters under 1 sun Illumination with Different Counter Electrodes and Electrolytes Based on 3D CdSe/CdS/ZnO Nanostructured Photoelectrode[a]

sample	V_{oc} (V)	J_{sc} (mA/cm^2)	FF (%)	efficiency (%)
Au/liquid electrolyte	0.684	16.50	45	5.08
C/liquid electrolyte	0.732	17.32	45	5.69
C/gel electrolyte	0.719	17.84	42	5.45

[a]5 mm × 5 mm cell size.

was the effect of the flammable and volatile solvent, which causes lowering of the cell performance and electrolyte leakage problem. The other was the chemical reaction of the redox couple with noble metal in counter electrode. Thus, we have investigated these effects sequentially in this study. In our system, the gel electrolytes exhibited lower cell efficiency (5.45%) when compared to the liquid cell's efficiency (5.69%) due to their lower electrolyte conductivity. The IPCE measurements were performed for two cells, and the results showed behaviors similar to $I-V$ results (Figure 7).

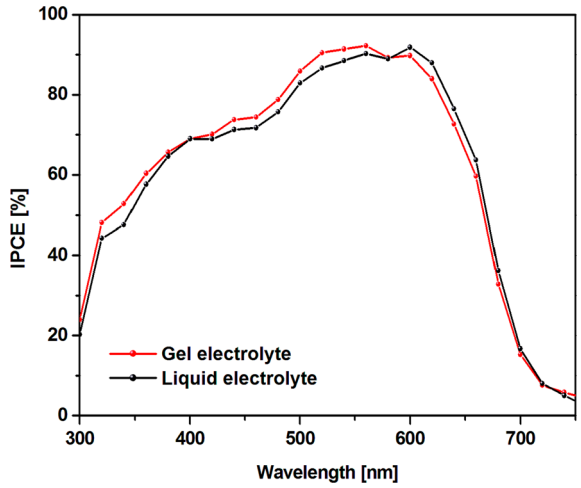

Figure 7. Incident photon to chemical efficiency (IPCE) measurement of the (red) gel electrolyte and (black) liquid electrolyte with three-dimensional CdSe/CdS/ZnO nanostructructure/electrolyte/Au counter electrode under 1 sun irradiation (cell dimension 5 mm × 5 mm).

Finally, with these three different QDSSC cells, we compared the stability of the cell under 1 sun irradiation conditions during the 5000 s. With the normalized current density measurements, we observed the remarkably enhanced stability of cell performance for the gel electrolyte employing the carbon CE-QDSSC system. This result is due to the efficient prohibition of poisoning at the counter electrode and to the stabilized gel electrolyte using the oligomer and nanocomposite. Such an improved performance of the optimized QDSSC indicates that the modified electrolyte and counter electrode can affect the long-term stability with lowering of the leakage and chemical corrosiveness.

CONCLUSION

In this study, we successfully improved the QDSSC cell stability using the oligomer-based gel electrolyte. With the lower molecular weight PEO, we replaced the methanol-based solvent of the polysulfide electrolyte and achieved solidification using the silica nanocomposite additives. The modified gel electrolyte showed comparable photo response properties as compared to those of the liquid electrolyte. In addition, we employed the carbon-based counter electrode to reduce the chemical reactions, which can affect to the cell performance and lead to degradation. Using the 1D CNT for charge transport and 2D RGO for highly reactive surface, the prepared counter electrode facilitates the electric conductivity. Additionally, the electrocatalytic properties can be enhanced by the nanosized Pt deposition on a carbon scaffold. As a result, the QDSSC cell was optimized for long-term stability and highly efficient light harvesting. The optimized cell exhibited 5.45% photon-to-electric conversion efficiency with long-term stability over 5000 s operation time.

AUTHOR INFORMATION

Corresponding Author

*E-mail: kyong@postech.ac.kr.

Notes

The authors declare no competing financial interest.

ACKNOWLEDGMENTS

This work was supported by the National Research Foundation of Korea (2013-R1A2A2A05-005344).

REFERENCES

(1) Grätzel, M. Photoelectrochemical Cells. *Nature* **2001**, *414*, 338−344.
(2) Hod, I.; Zaban, A. Materials and Interfaces in Quantum Dot Sensitized Solar Cells: Challenges, Advances and Prospects. *Langmuir* **2013**, *10*, 1021/la403768j.
(3) Jovanovski, V.; González-Pedro, V.; Giménez, S.; Azaceta, E.; Cabañero, G.; Grande, H.; Tena-Zaera, R.; Mora-Seró, I.; Bisquert, J. A Sulfide/Polysulfide-Based Ionic Liquid Electrolyte for Quantum Dot-Sensitized Solar Cells. *J. Am. Chem. Soc.* **2011**, *133*, 20156−20159.
(4) Wang, G.; Yang, X.; Qian, F.; Zhang, J. Z.; Li, Y. Double-Sided CdS and CdSe Quantum Dot Co-Sensitized ZnO Nanowire Arrays for Photoelectrochemical Hydrogen Generation. *Nano Lett.* **2010**, *10*, 1088−1092.
(5) Lee, Y.-L.; Lo, Y.-S. Highly Efficient Quantum-Dot-Sensitized Solar Cell Based on Co-Sensitization of CdS/CdSe. *Adv. Funct. Mater.* **2009**, *19*, 604−609.
(6) Kamat, P. V. Quantum Dot Solar Cells. Semiconductor Nanocrystals as Light Harvesters. *J. Phys. Chem. C* **2008**, *112*, 18737−18753.
(7) Shalom, M.; Buhbut, S.; Tirosh, S.; Zaban, A. Design Rules for High-Efficiency Quantum-Dot-Sensitized Solar Cells: A Multilayer Approach. *J. Phys. Chem. Lett.* **2012**, *3*, 2436−2441.
(8) Tak, Y.; Hong, S. J.; Lee, J. S.; Yong, K. Fabrication of ZnO/CdS Core/shell Nanowire Arrays for Efficient Solar Energy Conversion. *J. Mater. Chem.* **2009**, *19*, 5945−5951.
(9) Sun, B.; Hao, Y.; Guo, F.; Cao, Y.; Zhang, Y.; Li, Y.; Xu, D. Fabrication of Poly(3-hexylthiophene)/CdS/ZnO Core−Shell Nanotube Array for Semiconductor-Sensitized Solar Cell. *J. Phys. Chem. C* **2011**, *116*, 1395−1400.
(10) Li, D.-M.; Cheng, L.-Y.; Zhang, Y.-D.; Zhang, Q.-X.; Huang, X.-M.; Luo, Y.-H.; Meng, Q.-B. Development of Cu2S/carbon Composite Electrode for CdS/CdSe Quantum Dot Sensitized Solar Sell Modules. *Sol. Energy Mater. Sol. Cells* **2014**, *120*, 454−461.
(11) Wang, H.; Kubo, T.; Nakazaki, J.; Kinoshita, T.; Segawa, H. PbS-Quantum-Dot-Based Heterojunction Solar Cells Utilizing ZnO Nanowires for High External Quantum Efficiency in the Near-Infrared Region. *J. Phys. Chem. Lett.* **2013**, *4*, 2455−2460.
(12) Tachan, Z.; Shalom, M.; Hod, I.; Rühle, S.; Tirosh, S.; Zaban, A. PbS as a Highly Catalytic Counter Electrode for Polysulfide-Based Quantum Dot Solar Cells. *J. Phys. Chem. C* **2011**, *115*, 6162−6166.
(13) Lee, H.; Leventis, H. C.; Moon, S.-J.; Chen, P.; Ito, S.; Haque, S. A.; Torres, T.; Nüesch, F.; Geiger, T.; Zakeeruddin, S. M.; Grätzel, M.;

Nazeeruddin, M. K. PbS and US Quantum Dot-Sensitized Solid-State Solar Cells: "Old Concepts, New Results". *Adv. Funct. Mater.* **2009**, *19*, 2735−2742.
(14) Kim, H.; Seol, M.; Lee, J.; Yong, K. Highly Efficient Photoelectrochemical Hydrogen Generation Using Hierarchical ZnO/WOx Nanowires Cosensitized with CdSe/CdS. *J. Phys. Chem. C* **2011**, *115*, 25429−25436.
(15) Lee, Y.-L.; Huang, B.-M.; Chien, H.-T. Highly Efficient CdSe-Sensitized TiO_2 Photoelectrode for Quantum-Dot-Sensitized Solar Cell Applications. *Chem. Mater.* **2008**, *20*, 6903−6905.
(16) Santra, P. K.; Kamat, P. V. Mn-Doped Quantum Dot Sensitized Solar Cells: A Strategy to Boost Efficiency over 5%. *J. Am. Chem. Soc.* **2012**, *134*, 2508−2511.
(17) Law, M.; Greene, L. E.; Johnson, J. C.; Saykally, R.; Yang, P. Nanowire Dye-sensitized Solar Cells. *Nat. Mater.* **2005**, *4*, 455−459.
(18) Karageorgopoulos, D.; Stathatos, E.; Vitoratos, E. Thin ZnO Nanocrystalline Films for Efficient Quasi-solid State Electrolyte Quantum Dot Sensitized Solar Cells. *J. Power Sources* **2012**, *219*, 9−15.
(19) Zheng, Y.-Z.; Ding, H.; Liu, Y.; Tao, X.; Cao, G.; Chen, J.-F. In Situ Hydrothermal Growth of Hierarchical ZnO Nanourchin for High-efficiency Dye-sensitized Solar Cells. *J. Power Sources* **2014**, *254*, 153−160.
(20) Lu, F.; Cai, W.; Zhang, Y. ZnO Hierarchical Micro/Nanoarchitectures: Solvothermal Synthesis and Structurally Enhanced Photocatalytic Performance. *Adv. Funct. Mater.* **2008**, *18*, 1047−1056.
(21) Kim, H.; Yong, K. A Highly Efficient Light Capturing 2D (nanosheet)-1D (nanorod) Combined Hierarchical ZnO nanostructure for Efficient Quantum Dot Sensitized Solar Cells. *Phys. Chem. Chem. Phys.* **2013**, *15*, 2109−2116.
(22) Lee, Y.-L.; Chang, C.-H. Efficient Polysulfide Electrolyte for CdS Quantum Dot-sensitized Solar Cells. *J. Power Sources* **2008**, *185*, 584−588.
(23) Seo, H.; Wang, Y.; Uchida, G.; Kamataki, K.; Itagaki, N.; Koga, K.; Shiratani, M. Analysis on the Effect of Polysulfide Electrolyte Composition for Higher Performance of Si Quantum Dot-sensitized Solar Cells. *Electrochim. Acta* **2013**, *95*, 43−47.
(24) Chen, H.-Y.; Lin, L.; Yu, X.-Y.; Qiu, K.-Q.; Lü, X.-Y.; Kuang, D.-B.; Su, C.-Y. Dextran based Highly Conductive Hydrogel Polysulfide Electrolyte for Efficient Quasi-solid-state Quantum Dot-Sensitized Solar Cells. *Electrochim. Acta* **2013**, *92*, 117−123.
(25) Yu, Z.; Zhang, Q.; Qin, D.; Luo, Y.; Li, D.; Shen, Q.; Toyoda, T.; Meng, Q. Highly Efficient Quasi-solid-state Quantum-dot-sensitized Solar Cell based on Hydrogel Electrolytes. *Electrochem. Commun.* **2010**, *12*, 1776−1779.
(26) Seol, M.; Jang, J.-W.; Cho, S.; Lee, J. S.; Yong, K. Highly Efficient and Stable Cadmium Chalcogenide Quantum Dot/ZnO Nanowires for Photoelectrochemical Hydrogen Generation. *Chem. Mater.* **2013**, *25*, 184−189.
(27) O'Regan, B.; Lenzmann, F.; Muis, R.; Wienke, J. A Solid-State Dye-Sensitized Solar Cell Fabricated with Pressure-Treated P25−TiO_2 and CuSCN: Analysis of Pore Filling and IV Characteristics. *Chem. Mater.* **2002**, *14*, 5023−5029.
(28) Bach, U.; Lupo, D.; Comte, P.; Moser, J. E.; Weissortel, F.; Salbeck, J.; Spreitzer, H.; Gratzel, M. Solid-state Dye-sensitized Mesoporous TiO_2 Solar Cells with High Photon-to-electron Conversion Efficiencies. *Nature* **1998**, *395*, 583−585.
(29) Plass, R.; Pelet, S.; Krueger, J.; Grätzel, M.; Bach, U. Quantum Dot Sensitization of Organic−Inorganic Hybrid Solar Cells. *J. Phys. Chem. B* **2002**, *106*, 7578−7580.
(30) Kim, H.; Jeong, H.; An, T. K.; Park, C. E.; Yong, K. Hybrid-Type Quantum-Dot Cosensitized ZnO Nanowire Solar Cell with Enhanced Visible-Light Harvesting. *ACS Appl. Mater. Interfaces* **2012**, *5*, 268−275.
(31) Dualeh, A.; Moehl, T.; Nazeeruddin, M. K.; Grätzel, M. Temperature Dependence of Transport Properties of Spiro-MeOTAD as a Hole Transport Material in Solid-State Dye-Sensitized Solar Cells. *ACS Nano* **2013**, *7*, 2292−2301.
(32) Hu, M.; Sun, J.; Rong, Y.; Yang, Y.; Liu, L.; Li, X.; Forsyth, M.; MacFarlane, D. R.; Han, H. Enhancement of Monobasal Solid-state Dye-sensitized Solar Cells with Polymer Electrolyte Assembling Imidazolium Iodide-functionalized Silica Nanoparticles. *J. Power Sources* **2014**, *248*, 283−288.
(33) Singh, P. K.; Nagarale, R.; Pandey, S.; Rhee, H.; Bhattacharya, B. Present Status of Solid State Photoelectrochemical Solar Cells and Dye Sensitized Solar Cells using PEO-based Polymer Electrolytes. *Adv. Nat. Sci.: Nanosci. Nanotechnol.* **2011**, *2*, 023002−0230015.
(34) Chen, H.-W.; Chiang, Y.-D.; Kung, C.-W.; Sakai, N.; Ikegami, M.; Yamauchi, Y.; Wu, K. C. W.; Miyasaka, T.; Ho, K.-C. Highly Efficient Plastic-based Quasi-solid-state Dye-sensitized Solar Cells with Light-harvesting Mesoporous Silica Nanoparticles Gel-electrolyte. *J. Power Sources* **2014**, *245*, 411−417.
(35) Matsumoto, M.; Miyazaki, H.; Matsuhiro, K.; Kumashiro, Y.; Takaoka, Y. A Dye Sensitized TiO_2 Photoelectrochemical Cell Constructed with Polymer Solid Electrolyte. *Solid State Ionics* **1996**, *89*, 263−267.
(36) Shi, C.; Qiu, L.; Chen, X.; Zhang, H.; Wang, L.; Yan, F. Silica Nanoparticle Doped Organic Ionic Plastic Crystal Electrolytes for Highly Efficient Solid-State Dye-Sensitized Solar Cells. *ACS Appl. Mater. Interfaces* **2013**, *5*, 1453−1459.
(37) Wang, P.; Zakeeruddin, S. M.; Comte, P.; Exnar, I.; Grätzel, M. Gelation of Ionic Liquid-Based Electrolytes with Silica Nanoparticles for Quasi-Solid-State Dye-Sensitized Solar Cells. *J. Am. Chem. Soc.* **2003**, *125*, 1166−1167.
(38) Li, B.; Wang, L.; Kang, B.; Wang, P.; Qiu, Y. Review of Recent Progress in Solid-state Dye-Sensitized Solar Cells. *Sol. Energy Mater. Sol. Cells* **2006**, *90*, 549−573.
(39) Kang, M.-S.; Ahn, K.-S.; Lee, J.-W. Quasi-solid-state Dye-sensitized Solar Cells Employing Ternary Component Polymer-gel Electrolytes. *J. Power Sources* **2008**, *180*, 896−901.
(40) Kang, M.-S.; Kim, J. H.; Won, J.; Kang, Y. S. Oligomer Approaches for Solid-State Dye-Sensitized Solar Cells Employing Polymer Electrolytes. *J. Phys. Chem. C* **2007**, *111*, 5222−5228.
(41) Kim, J. H.; Kang, M.-S.; Kim, Y. J.; Won, J.; Park, N.-G.; Kang, Y. S. Dye-sensitized Nanocrystalline Solar Cells based on Composite Polymer Electrolytes Containing Fumed Silica Nanoparticles. *Chem. Commun.* **2004**, *14*, 1662−1663.
(42) Seol, M.; Youn, D. H.; Kim, J. Y.; Jang, J.-W.; Choi, M.; Lee, J. S.; Yong, K. Mo-Compound/CNT-Graphene Composites as Efficient Catalytic Electrodes for Quantum-Dot-Sensitized Solar Cells. *Adv. Energy Mater.* **2013**, *10*, 1002/aenm.201300775.
(43) Tak, Y.; Yong, K. Controlled Growth of Well-Aligned ZnO Nanorod Array Using a Novel Solution Method. *J. Phys. Chem. B* **2005**, *109*, 19263−19269.
(44) Seol, M.; Kim, H.; Tak, Y.; Yong, K. Novel nanowire array based highly efficient quantum dot sensitized solar cell. *Chem. Commun.* **2010**, *46*, 5521−5523.
(45) Seol, M.; Ramasamy, E.; Lee, J.; Yong, K. Highly Efficient and Durable Quantum Dot Sensitized ZnO Nanowire Solar Cell Using Noble-Metal-Free Counter Electrode. *J. Phys. Chem. C* **2011**, *115*, 22018−22024.
(46) Freitas, F. S.; Freitas, J. N. d.; Ito, B. I.; Paoli, M.-A. D.; Nogueira, A. F. Electrochemical and Structural Characterization of Polymer Gel Electrolytes Based on a PEO Copolymer and an Imidazolium-Based Ionic Liquid for Dye-Sensitized Solar Cells. *ACS Appl. Mater. Interfaces* **2009**, *1*, 2870−2877.
(47) Ren, Y.; Zhang, Z.; Fang, S.; Yang, M.; Cai, S. Application of PEO Based Gel Network Polymer Electrolytes in Dye-Sensitized Photoelectrochemical Cells. *Sol. Energy Mater. Sol. Cells* **2002**, *71*, 253−259.
(48) Kang, M.-S.; Kim, Y. J.; Won, J.; Kang, Y. S. Roles of Terminal Groups of Oligomer Electrolytes in Determining Photovoltaic Performances of Dye-sensitized Solar Cells. *Chem. Commun.* **2005**, *21*, 2686−2688.
(49) Stergiopoulos, T.; Bidikoudi, M.; Likodimos, V.; Falaras, P. Dye-sensitized Solar Cells Incorporating Novel Co(II/III) based-redox Electrolytes Solidified by Silica Nanoparticles. *J. Mater. Chem.* **2012**, *22*, 24430−24438.

(50) Wang, Q.; Moser, J.-E.; Grätzel, M. Electrochemical Impedance Spectroscopic Analysis of Dye-Sensitized Solar Cells. *J. Phys. Chem. B* **2005**, *109*, 14945−14953.
(51) Huo, Z.; Dai, S.; Wang, K.; Kong, F.; Zhang, C.; Pan, X.; Fang, X. Nanocomposite Gel Electrolyte with Large Enhanced Charge Transport Properties of an I^{-3}/I^{-} Redox Couple for Quasi-solid-state Dye-sensitized Solar Cells. *Sol. Energy Mater. Sol. Cells* **2007**, *91*, 1959−1965.
(52) Yong, Z.; Jin, Z.; Shuxin, T.; Lifang, W.; Lei, J.; Daoben, Z. TiO_2 Micro/nano-composite Structured Electrodes for Quasi-solid-state Dye-sensitized Solar Cells. *Nanotechnology* **2006**, *17*, 2090−2092.